Structural Biology and Molecular Biophysics
Cell Biology

A biochemical mechanism for Stu2/XMAP215-family microtubule polymerases

Reviewed Preprint
v1 • July 25, 2025
Not revised

Binnu Gangadharan, Daniel L Kober, Luke M Rice

Department of Biophysics, University of Texas Southwestern Medical Center, Dallas, United States • Department of Biochemistry, University of Texas Southwestern Medical Center, Dallas, United States

eLife Assessment

In their **important** manuscript, Gangadharan, Kober and Rice focus on how Stu2/XMAP215-family microtubule polymerases use their TOG domains to catalytically promote microtubule growth, testing whether their mechanism follows an enzyme-like kinetic model similar to that of actin polymerases. The authors integrate measurements including microtubule polymerization rates and TOG-tubulin binding kinetics to **convincingly** show that Stu2 follows an enzyme-like model where tight tubulin binding enables efficient polymerization, revealing a shared mechanism with actin polymerases despite their evolutionary divergence. This work will be of general interest to the cell biology and biophysics communities.

https://doi.org/10.7554/eLife.107818.1.sa3

Abstract

Defining quantitative biochemical mechanisms of microtubule dynamics and regulation is a current challenge. Stu2/XMAP215-family polymerases use tubulin-binding TOG domains to catalyze microtubule growth, but how polymerase activity results from the number and tubulin-binding properties of TOGs is not understood. We tested whether an enzyme-like biochemical model for the unrelated actin polymerase Ena/VASP could be applied to quantitatively relate Stu2 microtubule polymerase activity to the number of its TOGs and the rate constants governing their interactions with tubulin. Stu2 activity displayed enzyme-like characteristics consistent with the biochemical model: Stu2 stimulated microtubule growth rates with hyperbolic dependence on tubulin concentration, and the amount of Stu2 on the microtubule end did not vary with tubulin concentration (microtubule growth rate). Complementary measurements of TOG:tubulin binding revealed high affinity (10 nM) and slow dissociation (0.03 s^{-1}). The polymerase and binding measurements can be unified within the biochemical model: Stu2 operates with high efficiency, acting as a tubulin-shuttling antenna on the microtubule end that is primarily limited by the rate of tubulin:TOG association. Our work thus provides a quantitative biochemical mechanism for TOG-based polymerases. That unrelated microtubule and actin polymerases use the same enzyme-like mechanism provides an example of convergent evolution in the cytoskeleton.

Introduction

Microtubules (MTs) are dynamic polymers of αβ-tubulin (tubulin) that mediate essential cellular functions such as cell division, transport, and motility (Janke and Magiera, 2020). MT dynamics are regulated by multiple MT-associated proteins (MAPs) (Akhmanova and Steinmetz, 2015; Brouhard and Rice, 2018; Goodson and Jonasson, 2018; Gudimchuk and McIntosh, 2021). Defining and quantifying the biochemical mechanisms underlying MT dynamics and regulation is an ongoing challenge for the field.

Stu2/XMAP215-family proteins are conserved 'polymerases' (Gard and Kirschner, 1987; Ohkura et al., 1988) that catalyze MT growth using αβ-tubulin-binding TOG (Tumor Overexpressed Gene) domains (Al-Bassam et al., 2007; Ayaz et al., 2012; Brouhard et al., 2008)(**Fig. 1A**). All family members contain multiple, flexibly-linked TOG domains, but the domain organization and oligomerization state of these polymerases can vary across taxa (Al-Bassam and Chang, 2011; Slep, 2009)(**Fig. 1B**): fungal polymerases such as Stu2 (S. cerevisiae) and Alp14 (S. pombe) are homodimers containing two different TOG domains per monomer whereas metazoan polymerases like XMAP215 (X. laevis) and chTOG (H. sapiens) are monomers containing 5 (or possibly 6) different TOG domains. Despite years of study from multiple groups, a quantitative biochemical understanding of how these polymerases work has not yet been defined. Currently, two main classes of mechanism for polymerase activity have been proposed. Our group advanced a 'concentrating reactants' model in which catalytic polymerase activity results from linked TOG domains at the MT end recruiting unpolymerized tubulin, thereby increasing the effective concentration of tubulin and consequently the rate of tubulin:MT interactions(Ayaz et al., 2014; Ayaz et al., 2012; Geyer et al., 2018). Another group proposed a 'polarized unfurling' model (Nithianantham et al., 2018) in which polymerase activity results from a multi-step, multi-tubulin delivery process that postulates specific TOG:TOG contacts and distinct roles for different TOG domains; this model is based on structures of TOG:tubulin complexes but does not obviously explain why polymerase activity is catalytic. These two models represent very different views about how the polymerase might work and have different implications for thinking about TOG-based polymerase mechanism across taxa. Nevertheless, they both share a common limitation: neither quantitatively links polymerase activity to the number and tubulin-binding affinity/kinetics of TOG domains.

With the goal of providing a deeper and more general understanding of Stu2/XMAP215-family polymerase mechanism and whether it is conserved between homodimeric and monomeric family members, we sought to improve over current models by defining a quantitative relationship between the growth-promoting activity of a polymerase and the number and tubulin-binding properties of its TOG domains. We were inspired by prior work on Ena/VASP, an otherwise unrelated actin polymerase that appears to share a similar functional design with Stu2/XMAP215 polymerases: both polymerases contain multiple flexibly linked domains (**Figure 1C**) — TOGs in Stu2/XMAP215 and GAB/EVH2 in Ena/VASP — that preferentially interact with unpolymerized tubulin and actin, respectively (Ayaz et al., 2014; Ayaz et al., 2012; Ferron et al., 2007; Walders-Harbeck et al., 2002). In contrast to the MT polymerases, however, for the actin polymerase Ena/VASP there is a quantitative biochemical model that explains how its polymerase activity results from the number and actin-binding kinetics of its GAB domains (**Fig. 1D**) (Breitsprecher et al., 2011). Using Stu2 as a model, we tested whether the biochemical model for an actin polymerase could also be applied to explain the activity of MT polymerases.

The biochemical model (Breitsprecher et al., 2011) essentially views the polymerase as analogous to an enzyme that acts on the polymer end, using unpolymerized subunits as its substrate. We first showed that the growth-promoting activity of Stu2 displayed two characteristics required by the biochemical model (Breitsprecher et al., 2011): (i) a fixed concentration of Stu2

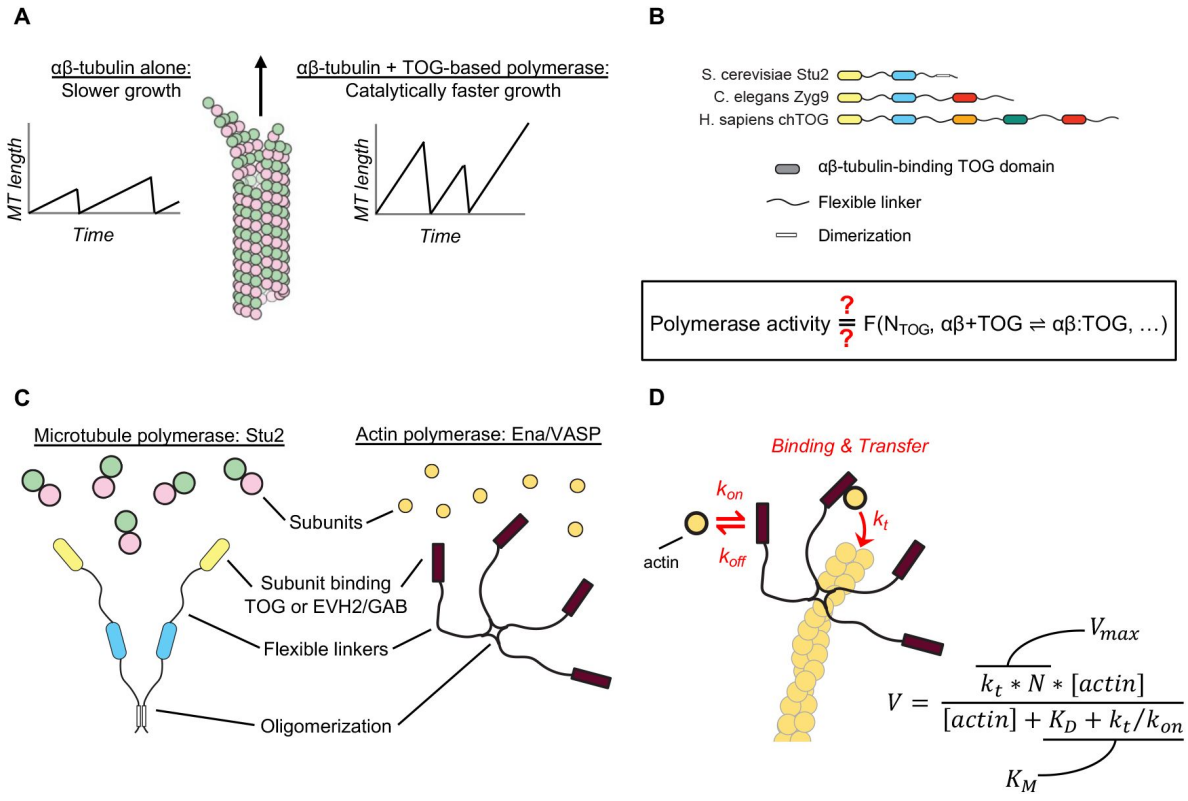

Figure 1.

Similarities between microtubule and actin polymerases suggest a shared mechanism.

A TOG-based microtubule polymerases catalyze faster microtubule growth.
B Schematic cartoons showing how the number of TOG domains and oligomerization state of TOG-based polymerases can vary in different organisms. Box: A biochemical understanding to explain how polymerase activity results from the number of TOG domains and the rate constants governing their interactions with tubulin has not been established.
C The microtubule polymerase Stu2 and the actin polymerase Ena/VASP may use a common mechanism: both polymerases are oligomers that contain subunit (tubulin or actin) binding domains connected by flexible linkers.
D Cartoon illustrating an enzyme-like mechanism (Breitsprecher et al., 2011) that quantitatively explains Ena/VASP activity in terms of the number of subunit binding domains (N), the rate constants governing their interactions with actin (k_{on}, k_{off}, K_D), and a transfer rate constant k_f that describes how fast the bound subunit is added to the polymer end. Equation: relationship between the Ena/VASP-mediated growth rate (V) and the number and biochemical properties of the actin-binding domains (Breitsprecher et al., 2011), annotated to indicate its similarity to the Michaelis-Menten equation.

stimulated MT elongation rate with hyperbolic dependence on tubulin concentration, consistent with enzyme-like action, and (ii) the amount of Stu2 on the MT end did not vary detectably with tubulin concentration, so variation in polymerase-stimulation of MT growth reflects something other than differential accumulation of the polymerase on the MT end. Finally, we directly measured the binding affinity and kinetics for TOG:tubulin interactions, revealing tighter than expected binding that is consistent with the measured dependence of polymerase activity on tubulin concentration.

The binding measurements and polymerase activity can be unified within the biochemical model, providing a quantitative understanding of how MT polymerase activity results from the number and tubulin binding kinetics of TOG domains. The results indicate that Stu2 operates with very high efficiency: the rate-limiting step in the mechanism is unpolymerized tubulin binding to a TOG domain, and once a TOG binds to an unpolymerized tubulin, that tubulin nearly always becomes incorporated into the MT. Nothing in the model requires a specific oligomerization state; given earlier data showing comparable activity for monomeric and dimeric "two TOG" variants of Stu2 (Geyer et al., 2018), the enzyme-like biochemical model should be broadly applicable to polymerases across taxa. Thus, Stu2/XMAP215-family polymerases function like tubulin-shuttling antennas that accelerate the arrival of unpolymerized tubulin to the MT end.

This kind of mechanism is more consistent with the 'concentrating reactants' mechanism we proposed previously (Ayaz et al., 2014). The biochemical model does not specify the mechanism of polymerase end localization, but there, too, Stu2/XMAP215 and Ena/VASP polymerases appear to share a common feature: both polymerases only localize to the growing end in the presence of unpolymerized subunits (Geyer et al., 2018; Hansen and Mullins, 2010) (in other words, end localization for both polymerases cannot be separated from polymerase activity). The similarity in mechanism between these two otherwise unrelated cytoskeletal polymerases provides an interesting example of convergent evolution. The common design principle likely indicates that localizing flexibly-linked subunit-binding domains to the growing polymer end is sufficient to generate polymerase activity.

Results

Does a similar modular organization in MT and actin polymerases reflect a common biochemical mechanism?

In seeking to define a biochemical mechanism to explain how Stu2/XMAP215-family MT polymerase activity results from the number and tubulin-binding properties of TOG domains (**Fig. 1B**), we were intrigued by apparent similarities between Stu2 and the actin polymerase Ena/VASP (**Fig. 1C**), for which a biochemical mechanism has already been defined (**Fig. 1D**) (Breitsprecher et al., 2011). Both Stu2 and Ena/VASP are oligomeric polymerases that contain multiple flexibly-linked domains (TOGs for Stu2/XMAP215 and GAB for Ena/VASP) that bind preferentially to unpolymerized tubulin and actin, respectively. We test here whether the model that quantitatively describes how Eva/VASP polymerase activity results from the number and biochemical properties of its actin-binding domains (**Figure 1D**) can also be used to provide a molecular understanding of Stu2 MT polymerase activity.

The biochemical model effectively considers the polymerase as analogous to an enzyme that acts on the polymer end and that uses unpolymerized subunits as its substrate. The biochemical model predicts a Michaelis-Menten-like (hyperbolic) dependence of polymerase-stimulated growth rate on subunit concentration, and it directly relates characteristics of polymerase activity - the apparent maximal stimulation of growth rate (V_{max}) and the concentration at which half-maximal stimulation is achieved (K_M) - to the number of TOG domains (N) and the rate constants for the underlying biochemical reactions: subunits associating/dissociating from a binding domain (k_{on},

k_{off}, K_D) or for being transferred from the binding domain to the growing end of the polymer (k_t) (**Figure 1C**). Prior *in vitro* measurements of Stu2/XMAP215-family polymerase activity (Brouhard et al., 2008; Cook et al., 2019; Farmer et al., 2021; Geyer et al., 2018; Podolski et al., 2014; Roostalu et al., 2015; Thawani et al., 2018; Widlund et al., 2011) have generally varied polymerase concentration at a fixed concentration of tubulin. The model being explored here considers tubulin as the substrate and consequently is most easily tested at a fixed concentration of polymerase using variable tubulin concentration. Thus, we first obtained new measurements to determine whether Stu2-stimulated growth at different tubulin concentrations showed enzyme-like characteristics, as required by the biochemical model.

Polymerase activity at variable tubulin concentrations follows Michaelis-Menten-like behavior, consistent with the biochemical model

We measured *in vitro* MT growth rates using a constant, roughly half-saturating amount of Stu2 (100 nM) at concentrations of yeast tubulin ranging from 0.4 to 1.4 μM. In addition to wild-type Stu2 (hereafter denoted Stu2(TOG1-TOG2) to indicate the identity of the two TOG domains per monomer), and with the goal of facilitating model fitting, we also measured two additional variants (**Figure 2A**): Stu2(TOG2-TOG2) has the TOG1 domain replaced by a second TOG2 domain, which simplifies the biochemistry by only having one type of TOG:tubulin interaction; Stu2(TOG1*-TOG2) has one TOG domain (TOG1) 'inactivated' (TOG1* denotes a variant unable to bind tubulin, achieved here using the R200A mutation (Ayaz et al., 2012)) to vary the number of active TOGs in the polymerase.

Stu2 increased microtubule growth rates (**Fig. 2B,C**), and the Stu2-mediated growth rate (**Fig. 2C**) followed Michaelis-Menten-like (hyperbolic) dependence on tubulin concentration (**Figure 2D**). The maximal activity of Stu2(TOG2-TOG2) was comparable to that of Stu2(TOG1-TOG2) (both constructs contain 4 active TOG domains) while the maximal activity of Stu2(TOG1*-TOG2) – a construct that only contains 2 active TOG domains - was roughly half that of the unmutated constructs (**Figure 2C,D**; corresponding V_{max} and K_M values for the three constructs are summarized in **Figure 2D**, box). These results are consistent with prior work on these constructs (Geyer et al., 2018). That all constructs showed enzyme-like dependence on tubulin concentration means that the data may be amenable to analysis using enzyme-like biochemical model. Hereafter, experiments used Stu2(TOG2-TOG2) and Stu2(TOG1*-TOG2) constructs to avoid having to account for different TOG:tubulin affinities in the model.

The amount of Stu2 on the MT end is independent of MT growth rate

To analyze the Stu2 measurements in the context of the biochemical model requires that the amount of Stu2 on the microtubule end does not vary with tubulin concentration. We therefore quantified the amount of Stu2 on the MT end at low (0.6 μM) and high (1.4 μM) concentrations of αβ-tubulin, using TIRF to visualize GFP-tagged Stu2 on the end of growing, unlabeled MTs. End-resident Stu2 was quantified by measuring the fluorescence intensity of the Stu2-GFP comet (**Figure 3A**). The measured intensity did not differ detectably between low and high tubulin concentrations (**Figure 3B**), indicating that the amount of Stu2 on the MT end does not depend on the concentration of αβ-tubulin (or, equivalently, on how fast the microtubule is growing).

The measurements reported thus far indicate that Stu2 polymerase activity shows enzyme-like characteristics that make it amenable to analysis using the biochemical model initially developed for Ena/VASP. Specifically, Stu2-stimulated MT growth depends hyperbolically on tubulin concentration (is Michaelis-Menten-like), and the amount of Stu2 on the MT end does not depend on tubulin concentration. In the biochemical model (**Fig. 2D**), the dependence of polymerase activity on tubulin concentration is given by the apparent K_M, which is defined by $K_M = K_D +$

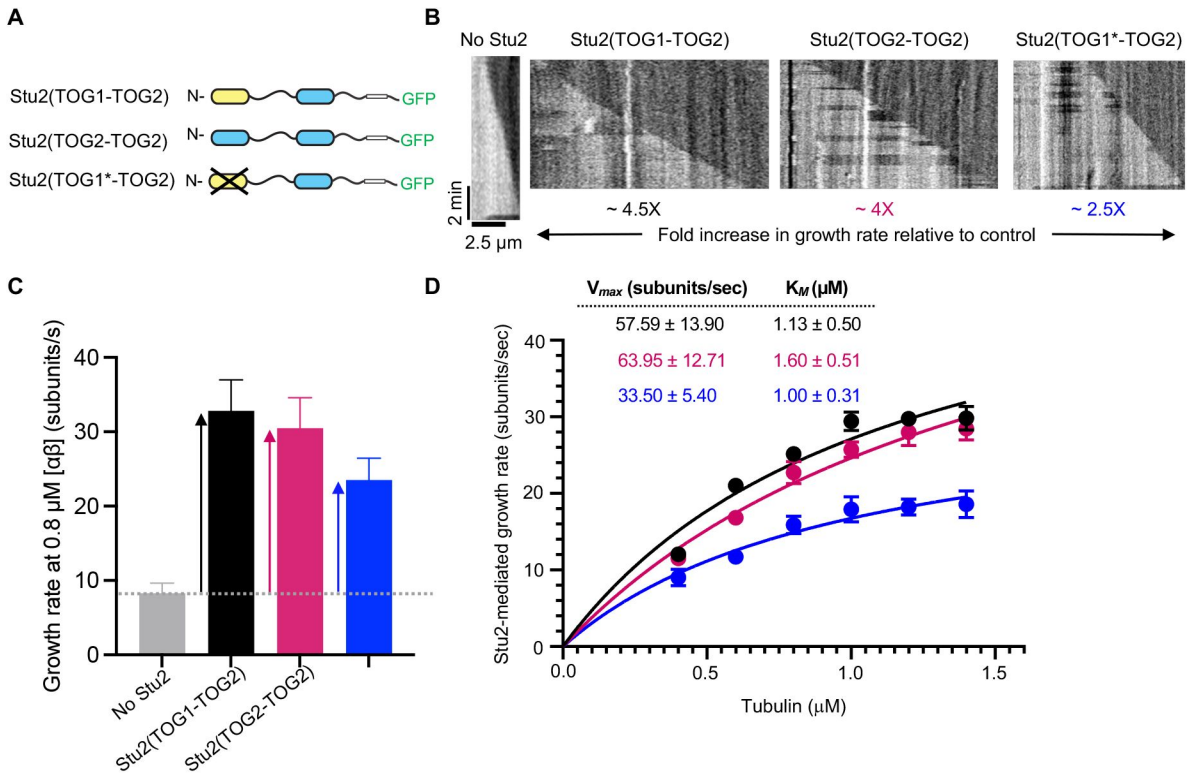

Figure 2.

Stu2 polymerase activity at different tubulin concentrations follows Michaelis-Menten kinetics, consistent with the biochemical model.

A Domain organization of Stu2 constructs used in this work.
B Representative kymographs from *in* vitro measurements of microtubule dynamics using the indicated constructs. TOG1* indicates a non-binding mutant (R200A mutation) that was used to vary the number of tubulin-binding TOG domains in the polymerase.
C Average MT growth rates from assays containing 0.8 µM yeast tubulin, without (No Stu2) or with 100 nM of the indicated Stu2 variant. Error bars represent SEM, n=25 for all. The dotted horizontal grey line shows the growth rate in control; vertical arrows indicate the Stu2-mediated growth rate.
D Stu2-mediated growth rates measured at multiple tubulin concentrations (filled circles), fit to the Michaelis-Menten equation. Error bars represent SEM, n=25 for all. The resulting V_{max} and K_M are shown in the inset table.

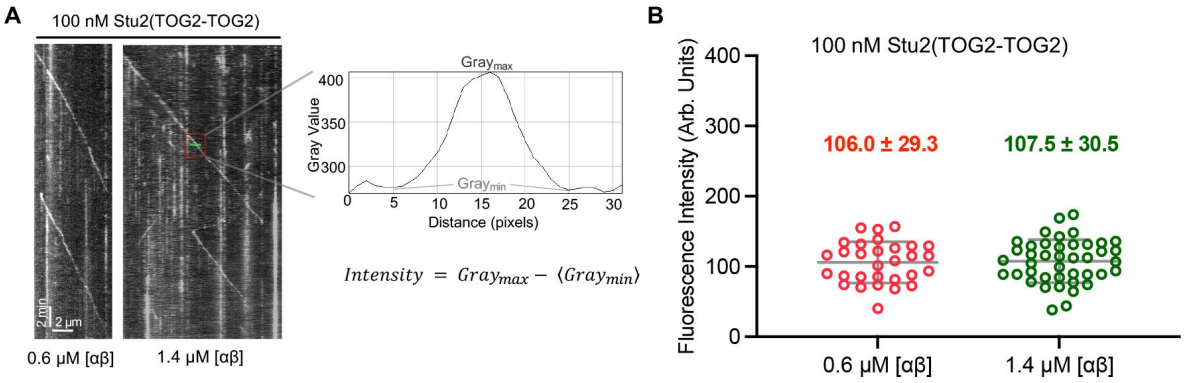

Figure 3.

The amount of Stu2 at the microtubule end is independent of microtubule growth rate.

A Representative kymographs for measurements from assays containing 100 nM Stu2(TOG2-TOG2) at the indicated tubulin concentrations (0.6 and 1.4 µM), monitored by TIRF microscopy. A minimum of 2-3 'comet' intensities were measured using intensity line scans as indicated for each growth episode.
B The fluorescence intensity at the microtubule end does not differ significantly (P=0.83) at low (0.6 µM; n=30) and high (1.4 µM; n=42) tubulin concentration. Similar fluorescent intensity values at both low and high tubulin concentrations indicate that the amount of Stu2 on the growing microtubule end does not vary with tubulin concentration. Bars indicate SD.

k_t/k_{on}. Accordingly, the concentration-dependence of polymerase activity could be dictated by the affinity of TOG:tubulin interactions ("affinity limited": $K_M \approx K_D$ and k_t/k_{on} negligeable), by the rate constants for TOG:tubulin association (k_{on}) and for transfer of a TOG-bound tubulin to the polymer end (k_t) ("kinetically limited": $K_M \approx k_t/k_{on}$ and K_M negligeable), or by a combination of both. To determine which regime is operative requires knowledge about the affinity and kinetics of TOG:tubulin interactions.

Tubulin binds rapidly and tightly to TOG2 (10 nM affinity) under the conditions of the polymerase assay

We previously measured the tubulin-binding affinity of Stu2-TOG1 (70 nM) and Stu2-TOG2 (160 nM) domains (Ayaz et al., 2014), but those equilibrium experiments did not provide information about the rates of TOG:tubulin association and dissociation. Moreover, those earlier measurements may not faithfully reflect the interactions present during the polymerase assay because they were made using different conditions of pH and ionic strength. We used Bio-layer Interferometry (BLI) to determine the affinity and kinetics of TOG2:tubulin interactions under buffer conditions close to those used for measuring polymerase activity (see Methods). Tubulin was site-specifically biotinylated on the C-terminus of β-tubulin using sortase-mediated protein splicing (Popp et al., 2007)(**Fig. 4A**) and then attached to streptavidin-coated chips. BLI measurements using wild-type TOG2 yielded a dose-dependent, saturable binding signal (**Fig. 4B,C**) and control measurements using TOG2* did not show evidence of binding (**Figure 4C**). Fitting the concentration-dependent amplitudes to a one-site binding model yielded an affinity of 8.9 nM for TOG2:tubulin binding (**Figure 4C**). Globally fitting single exponential curves to the association and dissociation phases yielded rate constants k_{on} (3.2×10^6 $M^{-1}s^{-1}$) and k_{off} (3×10^{-2} s^{-1}) with good fits (global $R^2 = 0.97$) (**Figure 4B**, box). Calculating the dissociation constant K_D from the measured rate constants ($K_D = k_{off}/k_{on}$) instead of from the amplitudes yielded a value of 9.6 nM, in good agreement with the amplitude-based determination. The ~10 nM TOG2:tubulin binding affinity is 16-fold stronger than the 160 nM affinity measured previously at higher ionic strength (Ayaz et al., 2014), and negligeable compared to the apparent K_M for polymerase activity. Thus, the TOG domains are effectively saturated with tubulin in the concentration range we measured, and consequently the polymerase must be kinetically limited by either the rate of TOG:tubulin binding or by the rate of TOG-mediated transfer to tubulin to the microtubule end.

Unifying measurements of polymerase activity and TOG:tubulin interaction kinetics

Are the biochemical measurements of TOG:tubulin interactions consistent with the polymerase measurements? The biochemical model provides a way to address this question because it provides a quantitative link between the enzyme-like characteristics (K_M, V_{max}) of polymerase activity and the tubulin-binding and transfer reactions carried out by the TOG domains. For example, the concentration-dependence of polymerase activity is dictated by the apparent K_M, which is defined by $K_M = K_D + k_t/k_{on}$ (**Fig. 2D**); in this expression k_t is the only unmeasured quantity, so we can solve for its value to obtain $k_t = 5.04$ s^{-1}. This transfer rate of ~5 s^{-1} for each TOG domain is close to the ~10 s^{-1} rate at which 'free' (not bound to a TOG) tubulins incorporate into growing microtubules in our assay (**Fig. 2C**). Similarly, the maximal polymerase activity is given by V_{max}, which is defined by $V_{max} = k_t$*N; having measured V_{max} and derived k_t, we can calculate the number of TOG domains to obtain N=12 total TOG domains for Stu2(TOG2-TOG2) and N=8 total TOG domains for Stu2(TOG1*-TOG2). Since each Stu2(TOG2-TOG2) dimer contains 4 binding-competent TOGs, N=12 indicates that approximately 3 TOG-TOG2 polymerases reside at the growing microtubule end in our assay. A similar calculation for Stu2(TOG1*-TOG2), which has 2 binding-competent TOGs, yields approximately 4 polymerases at the growing microtubule end. The estimate of 3-4 polymerases on the microtubule end at ~half-saturating concentrations of Stu2 is consistent with our earlier measurement of ~6 Stu2(TOG1-TOG2) molecules on the microtubule

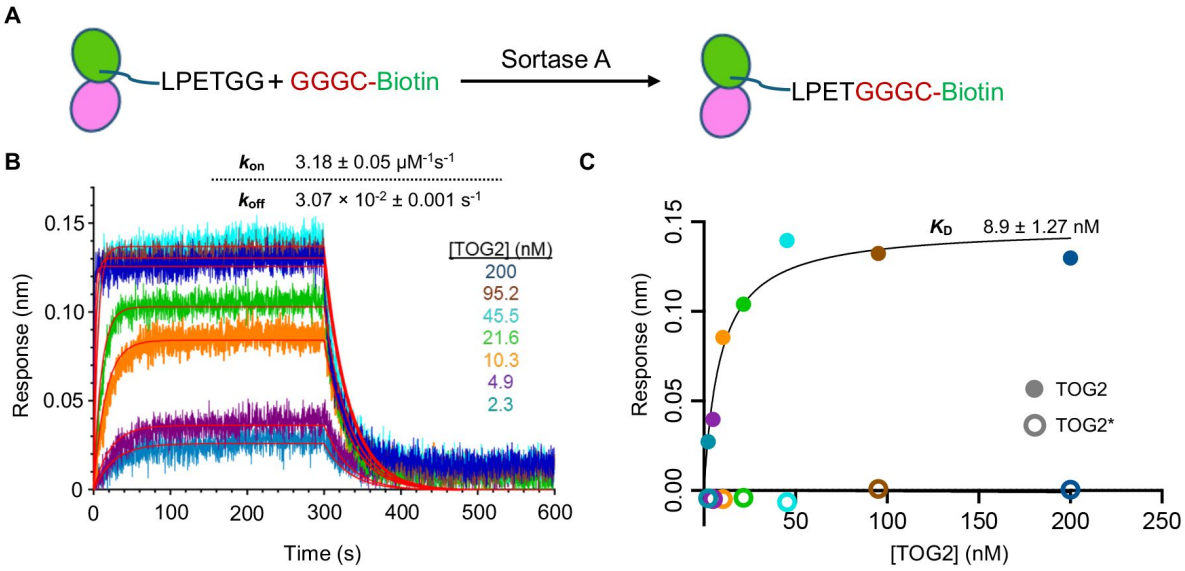

Figure 4.

Rate constants governing TOG:tubulin interactions under similar conditions to where polymerase activity was measured.

A Schematic of site-specific, sortase-mediated biotinylation of tubulin (see Methods). Yeast tubulin containing a sortase epitope (LPETGG) at the C-terminus of β tubulin was expressed and purified before reacting it with Sortase A and a separately prepared GGGC-Biotin peptide.

B Sensograms from biolayer interferometry measurements of different concentrations of TOG2 interacting with biotinylated tubulin immobilized on the sensor. Inset table: on- and off-rate constants obtained from globally fitting a 1:1 model to the data.

C Steady-state response for TOG2:tubulin binding plotted vs TOG2 concentration (filled circles) and fit to a 1:1 binding model (line). No response was observed for TOG2*, a mutant that does not bind tubulin. The dissociation constant obtained from the steady-state analysis (K_D = 9 nM) is consistent with the one calculated from kinetic measurements ($K_D = k_{off}/k_{on}$ = .0031/3.2 = 10 nM) and indicates a higher TOG:tubulin affinity than expected from prior measurements in different buffer conditions.

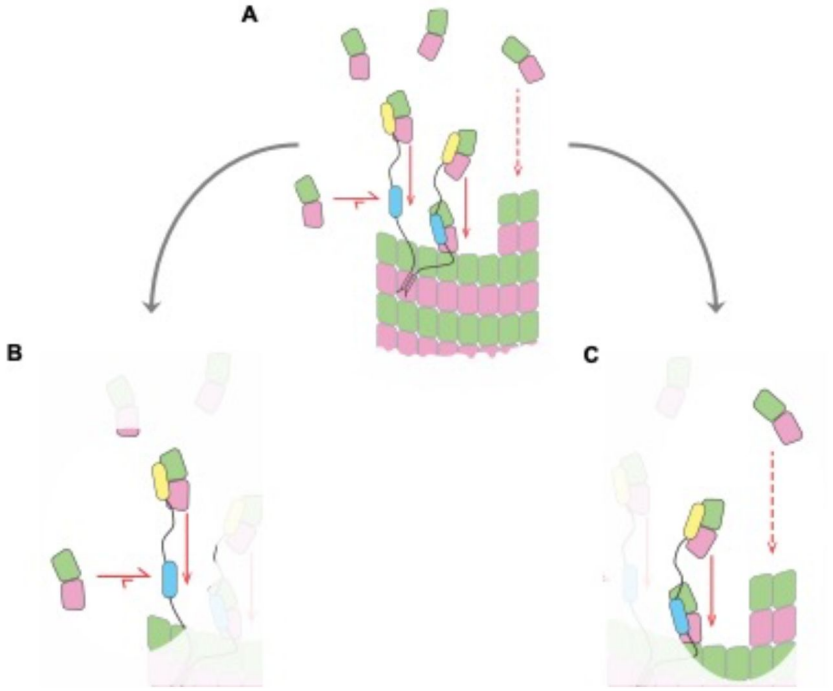

Figure 5.

Biochemical insights into the polymerase mechanism.

The cartoon summarizes the main insights obtained from the biochemical measurements and model. Only one polymerase is shown for clarity.

A Overview of the polymerase mechanism, illustrating the individual reactions: association and dissociation of TOG:tubulin complexes (horizontal arrows), 'transfer' of a TOG-bound tubulin to the microtubule end (solid vertical arrows), and uncatalyzed (polymerase-independent) association of unpolymerized tubulin with the microtubule end (dashed vertical arrow). Only one polymerase is shown for simplicity. Arrow lengths reflect the relative rates of different steps but are not to scale.

B The polymerase operates with high efficiency because the rate at which TOG-bound tubulins are transferred to the microtubule end (vertical downward arrow) greatly exceeds the rate at which TOG:tubulin complexes dissociate (horizontal leftward arrow). The polymerase is kinetically limited because the slowest step in the polymerase mechanism is tubulin binding to an 'empty' TOG (horizontal rightward arrow).

C The polymerase can achieve substantial rate enhancement because each TOG-bound tubulin is transferred to the microtubule end at a rate that is comparable to the uncatalyzed one (vertical downward arrows, and there can be multiple TOGs from multiple polymerases participating.

end under saturating conditions (Geyer et al., 2018). Thus, the measured enzyme-like characteristics of polymerase activity are consistent with and explained by the TOG:tubulin binding kinetics.

Discussion

The experiments and analyses described here provide a quantitative biochemical mechanism that explains the enzyme-like MT polymerase activity of Stu2 in terms of the number of TOG domains and their rate-constants for binding tubulin. High-affinity (~10 nM) TOG:tubulin interactions mean that once a TOG:tubulin complex forms, the TOG-bound tubulin will nearly always be delivered to the MT end (the 5 s^{-1} rate at which each TOG-bound tubulin is transferred to the MT end is >100-fold faster than the 3×10^{-2} s^{-1} rate at which tubulin dissociates from a TOG). The polymerase therefore operates with very high delivery efficiency. The high affinity of TOG:tubulin interactions, in particular that $K_D << K_M$, also means that Stu2 is kinetically limited.

Our measurements indicate that the rate of tubulin binding to TOG is most limiting for polymerase activity. Stu2 likely operates under a similar regime in cells, because the concentration of tubulin in yeast has been estimated to be on the order of 0.5 μM (Wethekam and Moore, 2023), which is comparable to the concentrations used in our in vitro experiments. Thus, Stu2 functions like a tubulin shuttling antenna that enhances capture of unpolymerized tubulin and accelerates its incorporation into the microtubule end.

Nothing in the biochemical model specifies how the tubulin-binding TOG domains need to be linked beyond that they be linked flexibly. Thus, the model should not be limited to homodimeric polymerases such as Stu2: it should apply equally well to monomeric polymerases that contain different numbers of TOG domains such as Zyg9 (3 TOGs) or XMAP215 and chTOG (5 TOGs). For any given polymerase, the overall activity will in general be determined by several factors. The number of tubulin-binding TOG domains and how many polymerases accumulate on the microtubule end together dictate the total number of TOG domains available to shuttle/deliver tubulin. The affinity and kinetics of TOG:tubulin interactions will determine the proportional contributions to polymerase activity from different TOGs, with lower affinity or slower binding TOGs contributing proportionally less than higher affinity, faster binding TOGs (e.g. (Widlund et al., 2011)). In addition to the polymerase-intrinsic factors above, whether a given polymerase is affinity or kinetically limited will also depend on the concentration of tubulin, which influences the rates of tubulin:TOG and tubulin:microtubule binding.

In summary, we showed that the same enzyme-like biochemical model can explain the activity of otherwise unrelated microtubule and actin polymerases: each polymerase resides at the polymer end and functions like a shuttling antenna, using multiple flexibly-linked actin or tubulin binding domains to capture and accelerate delivery of unpolymerized subunits to the polymer end. For the Stu2/XMAP215 microtubule polymerases, this is to our knowledge the first time that the polymerase activity has been quantitatively explained in terms of the number of TOG domains and their tubulin-binding rate constants. That two otherwise unrelated cytoskeletal polymerases share the same mechanism provides an interesting example of convergent evolution.

Materials and Methods

Plasmid construction

Plasmids expressing wild-type αβ yeast tubulin as well as polymerization blocked tubulin, LR1 (β: T175R,V179R) were previously described (Ayaz et al., 2012; Johnson et al., 2011). For sortase mediated peptide ligation, a sortase recognition sequence (LPETGG) was added to polymerization blocked tubulin at its C-terminus. The Stu2 variants - TOG1-TOG2, TOG2-TOG2, and TOG1*-TOG2 - were expressed using the pHAT vector, which includes an N-terminal HIS tag, a C-terminal eGFP sequence and Strep-tag, as previously described (Geyer et al., 2015; Geyer et al., 2018). Stu2-TOG2 (318–560) expressed from pET15b with a N-terminal HIS tag (Ayaz et al., 2012). All constructs were confirmed by DNA sequencing.

Protein expression and purification

Wild-type and polymerization-blocked αβ-tubulin were purified from inducibly overexpressing strains of *Saccharomyces cerevisiae* using Ni-affinity and anion exchange chromatography as described previously (Ayaz et al., 2012; Johnson et al., 2011). Purified tubulin samples were stored in 10 mM K-PIPES pH 6.9, 2 mM MgSO4, 1 mM EGTA with 50 µM GTP. Stu2 variants (TOG1-TOG2, TOG2-TOG2, TOG1*-TOG2) were overexpressed in *E. coli* using Arctic Express Cells using 0.5 mM IPTG for 24 hrs at 12 °C. Cell pellets were resuspended in lysis buffer (50 mM sodium phosphate dibasic and monobasic mix, 300 mM NaCl, 40 mM imidazole, 5% glycerol), PMSF was added to 1 mM final concentration and cells were lysed using a microfluidizer. Crude lysate was clarified by centrifugation before loading onto a His60 Superflow Column (Clontech). Column-bound proteins were eluted in Ni-elution buffer (lysis buffer + 300 mM imidazole). Pooled elution fractions were loaded onto a Strep-Tactin Superflow column (IBA, Germany) and eluted in Strep-elution buffer (RB100 + 10 mM desthiobiotin). Eluted samples were buffer exchanged into RB100 with 2 mL, 7K MWCO Zeba spin desalting columns (Thermo Scientific) for storage. Stu2-TOG2 (318-560) was overexpressed in *E. coli* and purified using a combination of Ni affinity and cation exchange chromatography as described previously (Geyer et al., 2015). Eluted samples were buffer exchanged into RB100 (25 mM Tris pH 7.5, 100 mM NaCl, 1 mM MgCl2, 1 mM EGTA) or dynamics assay buffer (90 mM PIPES, 10 mM NaCl, 1 mM MgCl2, 1 mM EGTA, 50 µM GTP), depending on the assays and flash frozen.

In vitro microtubule dynamics assay

Microtubule dynamics were imaged by either differential interference contrast microscopy (DIC) or total internal reflection fluorescence (TIRF) microscopy as previously described (Geyer et al., 2018). Briefly, assay chambers were assembled from slides, coverslips, and double sticky tape. The chambers were incubated with 5 mg/ml neutravidin (Sigma) and blocked using 1% F-127 Pluronic acid for 10 mins each. The chambers were then rinsed with BRB80 (80 mM PIPES pH 6.9, 1 mM MgCl2, 1 mM EGTA) followed by 10 min incubation with GMPCPP seeds made from brain tubulin (5% biotinylated, PurSolutions). Chambers were rinsed again with BRB80 and samples containing tubulin, Stu2 in 1X PEM (90 mM K-PIPES, 1 mM EGTA, 1 mM MgSO4) + 0.1 mg/ml bovine serum albumin (BSA) + 1 mM GTP were flowed into the same and immediately sealed with VALAP. Microtubule dynamics were measured manually by creating kymographs with ImageJ (Edelstein et al., 2010) and analyzed as previously described (Geyer et al., 2018)

End intensity measurements

To measure if there is a steady amount of polymerase at the growing MT end, the MT were imaged by TIRF. Flow chambers were prepared as stated in the previous section with addition of antifade agents (glucose, glucose oxidase, and catalase). Stu2 concentration was held constant at 100 nM while WT tubulin was used at 0.6µM and 1.4µM.

All imaging conditions such as exposure time, imaging angle were kept as identical as possible between two ranges of tubulin. Kymographs were created in ImageJ. For a given kymograph, intensities were measured at three different points of a growing MT (**Fig. 3A**) by drawing a uniform length line across each of those points and using the plot profile feature in ImageJ. The maximum and minimum gray values (intensity) for each plot were manually subtracted and analyzed using GraphPad Prism 10.2.

Bio-layer interferometry

We used sortase-mediated protein splicing to selectively label polymerization-blocked tubulin at the C-terminus of β-tubulin. GGGC peptide (Genscript) was incubated with a 20-fold molar excess of EZ-Link™ Maleimide-PEG2-Biotin (MPB) at room temperature. The reaction was quenched with 100 mM DTT after 2 hours. This biotinylated peptide provides the substrate for sortase-mediated labeling of tubulin. Labeling of polymerase-blocked tubulin was carried at room temperature for 30 minutes, with 50-fold molar excess of GGGC-MPB and 1.6-fold molar excess of sortase to polymerization-blocked tubulin, in sortase buffer (20 mM Tris pH 7.5, 125 mM NaCl, 1 mM TCEP, 0.01 mM $CaCl_2$ and 50 nM GTP). The reaction product was purified again using ion exchange chromatography to get rid of free peptides. The labeled blocked tubulin was confirmed using mass spectrophotometry.

BLI binding measurements were performed using Streptavidin (SA) biosensors on an OctetR8 instrument (Sartorius, Germany). The assay buffer consisted of 90 mM PIPES, 10 mM NaCl, 1 mM $MgCl_2$, 1 mM EGTA, 1 mM GTP, 0.1% BSA and 0.005% triton X-100. (BSA and triton X-100 were added to reduce non-specific binding to the biosensors). Biotinylated polymerization-blocked tubulin was immobilized on SA biosensors, which were then washed and dipped into wells containing TOG2 at concentrations ranging from 2.3 to 200 nM. The response level during immobilization was kept below 1 nm to minimize avidity-like artifacts. The association step lasted 300 seconds and was followed by a dissociation step, where the biosensor was moved into a well containing assay buffer, lasting 300 seconds. Data were double reference-subtracted using the signal from an unloaded pin dipped into TOG2 and a pin loading with LR1-457 dipped into assay buffer without TOG2. Association and dissociation rates were determining using a 1:1 binding mode analysis with the Octet BLI Discovery 13.0 (Orthwein et al., 2021).

Mathematical model for Stu2 mediated microtubule elongation

In this study, we adapted the Ena/VASP model for Stu2, as previously described (Breitsprecher et al., 2011). Briefly, the saturation dependence curve for tubulin shown in **Figure 2D** is reminiscent of the Michaelis-Menten model ($V=V_{max}[S]/K_M+[S]$) for enzyme kinetics with an assumption that each growing MT tip is associated with a few TOG domains, N. These domains are responsible for capturing tubulin with a rate constant k_{on} and transferring it onto the MT growing end with rate k_t. The tubulin can also be released back into the solution with an off rate k_{off}. Briefly, when we fit the MT elongation data with a Michaelis-Menten model, K_M corresponds to K_D+k_t/k_{on} and V_{max} corresponds to k_tN. By solving for the apparent K_M using K_D and k_{on}, we estimated k_t, which was then used to determine the value of 'N' for different Stu2 variants. The data were analyzed using GraphPad Prism 10.2.

Acknowledgements

We thank E. Bonventre, R. Chen, and L. McCormick for critical feedback on the manuscript. This work was supported by grants from the NIH: R01GM098543 and R35GM156385 to LMR, and R00GM141261 and R01GM155152 to DLK.

References

Akhmanova A., Steinmetz M.O. (2015) **Control of microtubule organization and dynamics: two ends in the limelight** *Nat Rev Mol Cell Biol* **16**:711–726 Google Scholar

Al-Bassam J., Chang F. (2011) **Regulation of microtubule dynamics by TOG-domain proteins XMAP215/Dis1 and CLASP** *Trends Cell Biol* **21**:604–614 Google Scholar

Al-Bassam J., Larsen N.A., Hyman A.A., Harrison S.C. (2007) **Crystal structure of a TOG domain: conserved features of XMAP215/Dis1-family TOG domains and implications for tubulin binding** *Structure* **15**:355–362 Google Scholar

Ayaz P., Munyoki S., Geyer E.A., Piedra F.A., Vu E.S., Bromberg R., Otwinowski Z., Grishin N.V., Brautigam C.A., Rice L.M. (2014) **A tethered delivery mechanism explains the catalytic action of a microtubule polymerase** *eLife* **3**:e03069 https://doi.org/10.7554/eLife.03069 | Google Scholar

Ayaz P., Ye X., Huddleston P., Brautigam C.A., Rice L.M. (2012) **A TOG:alphabeta-tubulin complex structure reveals conformation-based mechanisms for a microtubule polymerase** *Science* **337**:857–860 Google Scholar

Breitsprecher D., Kiesewetter A.K., Linkner J., Vinzenz M., Stradal T.E., Small J.V., Curth U., Dickinson R.B., Faix J. (2011) **Molecular mechanism of Ena/VASP-mediated actin-filament elongation** *EMBO J* **30**:456–467 Google Scholar

Brouhard G.J., Rice L.M. (2018) **Microtubule dynamics: an interplay of biochemistry and mechanics** *Nat Rev Mol Cell Biol* **19**:451–463 Google Scholar

Brouhard G.J., Stear J.H., Noetzel T.L., Al-Bassam J., Kinoshita K., Harrison S.C., Howard J., Hyman A.A. (2008) **XMAP215 is a processive microtubule polymerase** *Cell* **132**:79–88 Google Scholar

Cook B.D., Chang F., Flor-Parra I., Al-Bassam J. (2019) **Microtubule polymerase and processive plus-end tracking functions originate from distinct features within TOG domain arrays** *Mol Biol Cell* **30**:1490–1504 Google Scholar

Edelstein A., Amodaj N., Hoover K., Vale R., Stuurman N. (2010) **Computer control of microscopes using microManager** *Curr Protoc Mol Biol* **Chapter 14**:Unit14.20 Google Scholar

Farmer V., Arpag G., Hall S.L., Zanic M. (2021) **XMAP215 promotes microtubule catastrophe by disrupting the growing microtubule end** *J Cell Biol* **220** Google Scholar

Ferron F., Rebowski G., Lee S.H., Dominguez R. (2007) **Structural basis for the recruitment of profilin-actin complexes during filament elongation by Ena/VASP** *EMBO J* **26**:4597–4606 Google Scholar

Gard D.L., Kirschner M.W. (1987) **A microtubule-associated protein from Xenopus eggs that specifically promotes assembly at the plus-end** *J Cell Biol* **105**:2203–2215 Google Scholar

Geyer E.A., Burns A., Lalonde B.A., Ye X., Piedra F.A., Huffaker T.C., Rice L.M. (2015) **A mutation uncouples the tubulin conformational and GTPase cycles, revealing allosteric control of microtubule dynamics** *eLife* **4**:e10113 https://doi.org/10.7554/eLife.10113 | Google Scholar

Geyer E.A., Miller M.P., Brautigam C.A., Biggins S., Rice L.M. (2018) **Design principles of a microtubule polymerase** *eLife* **7** Google Scholar

Goodson H.V., Jonasson E.M. (2018) **Microtubules and Microtubule-Associated Proteins** *Cold Spring Harb Perspect Biol* **10** Google Scholar

Gudimchuk N.B., McIntosh J.R. (2021) **Regulation of microtubule dynamics, mechanics and function through the growing tip** *Nat Rev Mol Cell Biol* **22**:777–795 Google Scholar

Hansen S.D., Mullins R.D. (2010) **VASP is a processive actin polymerase that requires monomeric actin for barbed end association** *J Cell Biol* **191**:571–584 Google Scholar

Janke C., Magiera M.M. (2020) **The tubulin code and its role in controlling microtubule properties and functions** *Nat Rev Mol Cell Biol* **21**:307–326 Google Scholar

Johnson V., Ayaz P., Huddleston P., Rice L.M. (2011) **Design, overexpression, and purification of polymerization-blocked yeast alphabeta-tubulin mutants** *Biochemistry* **50**:8636–8644 Google Scholar

Nithianantham S., Cook B.D., Beans M., Guo F., Chang F., Al-Bassam J. (2018) **Structural basis of tubulin recruitment and assembly by microtubule polymerases with tumor overexpressed gene (TOG) domain arrays** *eLife* **7** Google Scholar

Ohkura H., Adachi Y., Kinoshita N., Niwa O., Toda T., Yanagida M. (1988) **Cold-sensitive and caffeine-supersensitive mutants of the Schizosaccharomyces pombe dis genes implicated in sister chromatid separation during mitosis** *EMBO J* **7**:1465–1473 Google Scholar

Orthwein T., Huergo L.F., Forchhammer K., Selim K.A. (2021) **Kinetic Analysis of a Protein-protein Complex to Determine its Dissociation Constant (K(D)) and the Effective Concentration (EC(50)) of an Interplaying Effector Molecule Using Bio-layer Interferometry** *Bio Protoc* **11**:e4152 Google Scholar

Podolski M., Mahamdeh M., Howard J. (2014) **Stu2, the budding yeast XMAP215/Dis1 homolog, promotes assembly of yeast microtubules by increasing growth rate and decreasing catastrophe frequency** *J Biol Chem* **289**:28087–28093 Google Scholar

Popp M.W., Antos J.M., Grotenbreg G.M., Spooner E., Ploegh H.L. (2007) **Sortagging: a versatile method for protein labeling** *Nat Chem Biol* **3**:707–708 Google Scholar

Roostalu J., Cade N.I., Surrey T. (2015) **Complementary activities of TPX2 and chTOG constitute an efficient importin-regulated microtubule nucleation module** *Nat Cell Biol* **17**:1422–1434 Google Scholar

Slep K.C. (2009) **The role of TOG domains in microtubule plus end dynamics** *Biochem Soc Trans* **37**:1002–1006 Google Scholar

Thawani A., Kadzik R.S., Petry S. (2018) **XMAP215 is a microtubule nucleation factor that functions synergistically with the gamma-tubulin ring complex** *Nat Cell Biol* **20**:575–585 Google Scholar

Walders-Harbeck B., Khaitlina S.Y., Hinssen H., Jockusch B.M., Illenberger S. (2002) **The vasodilator-stimulated phosphoprotein promotes actin polymerisation through direct binding to monomeric actin** *FEBS Lett* **529**:275–280 Google Scholar

Wethekam L.C., Moore J.K. (2023) **Tubulin isotype regulation maintains asymmetric requirement for alpha-tubulin over beta-tubulin** *J Cell Biol* **222** Google Scholar

Widlund P.O., Stear J.H., Pozniakovsky A., Zanic M., Reber S., Brouhard G.J., Hyman A.A., Howard J. (2011) **XMAP215 polymerase activity is built by combining multiple tubulin-binding TOG domains and a basic lattice-binding region** *Proc Natl Acad Sci U S A* **108**:2741–2746 Google Scholar

Author information

Binnu Gangadharan
Department of Biophysics, University of Texas Southwestern Medical Center, Dallas, United States

Daniel L Kober
Department of Biochemistry, University of Texas Southwestern Medical Center, Dallas, United States
ORCID iD: 0000-0001-8657-9348

Luke M Rice
Department of Biophysics, University of Texas Southwestern Medical Center, Dallas, United States, Department of Biochemistry, University of Texas Southwestern Medical Center, Dallas, United States
ORCID iD: 0000-0001-6551-3307

For correspondence: luke.rice@utsouthwestern.edu

Editors

Reviewing Editor
Kassandra Ori-McKenney
University of California, Davis, United States of America

Senior Editor
David Ron
University of Cambridge, Cambridge, United Kingdom

Reviewer #1 (Public review):

This study by Gangadharan and colleagues provides significant progress towards a quantitative biochemical mechanism for Stu2 polymerase activity. A key conceptual advance

is the novel application of an enzyme-like model, initially developed for the actin polymerase Ena/VASP, to Stu2.

New refined affinity measurements for a Stu2 TOG domain using Bio-layer interferometry show more than an order of magnitude higher affinity of TOG domains to tubulin compared to previously published reports.

The findings reinforce the "concentrating reactants" or, more specifically, for TOG-domain proteins, the "tubulin-shuttling antenna" model, compared to the "polarized unfurling" model, a more speculative structural hypothesis.

The manuscript builds upon a series of previous manuscripts that showcase the profound intellectual engagement with microtubule polymerization mechanisms by TOG-domain proteins from the Rice lab, a thought leader in microtubule polymerization for over a decade.

Minor remarks:

(1) A major new experimental finding of this paper is the affinity of TOG domains, which is more than an order of magnitude lower (10 nM) than previous measurements from the same lab (~200 nM). The authors attribute this change to ionic strength differences between buffer conditions, citing the lab's previous work (Ayaz et al., 2014). This argument left me contemplating what the buffer conditions are in both experiments, and I wonder if other readers would feel the same. After going down the rabbit hole, I believe the difference in ionic strength is ~2.3 fold, and at least on the back of my envelope, this works out beautifully with the measured differences in affinities. A short version of this argument may strengthen the manuscript.

(2) I am wondering if there may be an alternative explanation to tubulin binding by TOG being the kinetically rate-limiting step for polymerase function:

TOG + Tubulin ⇌ TOG:Tubulin (fast binding rate, high-affinity binding)
TOG:Tubulin + MT_end → TOG:MT (tubulin is incorporated into MT, fast transfer rate)
The binding rate is 3/s, and the transfer rate is 5/s.

I was wondering if the following step should be considered, which involves a conformational change of tubulin (e.g., straightening) TOG:MT → TOG + MT (rate-limiting straightening and unbinding of TOG from the lattice).

Presumably, the affinity of TOGs for straight tubulin is practically zero for the purpose of this discussion, as there is no lattice binding, which means unbinding is likely very rapid; however, straightening may be the rate-limiting factor here.

In theory, straightening should also be rapid; however, we lack measurements of how fast or slow this step occurs within the context of a TOG domain, which presumably skews the process towards curved tubulin.

A hypothetical Stu2, when bound to the microtubule end and with the TOG domain not disengaged from tubulin, would not permit the processivity of that molecule or the binding of a new molecule.
To emphasize the importance of unbinding, when it is not efficient, as reported for the T238 mutant that results in Stu2 lattice binding (Geyer et al., 2018), the polymerase becomes inefficient.

https://doi.org/10.7554/eLife.107818.1.sa2

Reviewer #2 (Public review):

Summary:

The manuscript from the Rice lab by Gangadharan et al. investigates the polymerization mechanism of the yeast microtubule polymerase Stu2. The lab has published a number of articles demonstrating the structural basis by which the two TOG domains of Stu2 each bind free tubulin heterodimers, and has developed a tethered polymerization model by which the TOG domains drive polymerization by shuttling those tubulin subunits onto the microtubule plus end. A second model was proposed by Nithianantham et al. (eLife, 2018) based on a closed-to-open transitional state in which Stu2 unfurls and loads two longitudinally associated tubulin heterodimers onto the microtubule plus end. While the second model is not directly tested, the current work aims to further characterize/model the tethered polymerization model using a kinetic framework developed by Breitsprecher et al. for Ena/VASP actin polymerization activity, using a model that is enzymatic (EMBO J., 2011). The general architecture and function of Ena/VASP on actin polymerization versus Stu2 on microtubule polymerization is a reasonable relation and hits upon, as the authors note, potential convergent mechanistic evolution across distinct cytoskeletal networks. The model effectively treats tubulin as the substrate, and the polymerized microtubule plus end as the product. If Stu2 is "enzymatic" in this framework, the model predicts it would behave with Michaelis-Menten kinetics, that there would a Vmax, and polymerase activity would either be "affinity limited" by TOG:tubulin affinity (KD) and/or "kinetically limited" by TOG:tubulin association (Kon) and transfer of tubulin to the microtubule plus end (Kt). The authors find that the Brietsprecher model works well for Stu2 activity, and that Stu2 best aligns with a "kinetically limited" model. The work is interesting and adds to the growing elucidation of the Stu2 microtubule polymerase model. While yeast microtubule polymerases are somewhat distinct in their architecture, there is significant overlap that findings from the manuscript can be utilized to inform the mechanisms of larger, more complex microtubule polymerases such as human ch-TOG.

Strengths:

The manuscript invokes the enzymatic model of Breitsprecher et al. used for Ena/VASP and conducts an elegant series of (mostly established) experiments to determine whether Stu2 microtubule polymerase activity aligns with the model, which they conclude does align, supported by the data/results obtained.

Weaknesses:

The authors used biolayer interferometry to measure TOG:tubulin affinity. The affinities obtained were significantly higher than the lab obtained in an earlier publication using analytical ultracentrifugation. While differences in buffer and salt conditions may underlie these differences, additional runs using comparable buffer systems, or the use of a third independent assay to measure affinities, would have added rigor.

The discussion could be expanded to better compare and contrast the results with both existing polymerase models introduced in the introduction, as well as expanded to look at reversible enzymatic activity (microtubule depolymerization at low to zero tubulin concentrations) and microtubule plus versus minus end activity.

https://doi.org/10.7554/eLife.107818.1.sa1

Reviewer #3 (Public review):

Summary:

This study by Gangadharan and colleagues seeks to establish a quantitative biochemical model for the microtubule polymerase activity of Stu2. Stu2 is the budding yeast member of the XMAP215 protein family, which is broadly conserved across eukaryotes. XMAP215 proteins play a wide variety of important roles in cells, and these are attributed to effects on microtubule dynamics. Many studies over the last ~20 years have shown that XMA215 proteins selectively associate with microtubule ends, where they increase rates of microtubule assembly and disassembly. More recently, structural biology and biochemical studies by the authors and other groups have shown that the multiple TOG domains on XMAP215 proteins are tubulin-binding domains that selectively bind to curved tubulin, which is present in solution and at microtubule ends, but not to straight tubulin which is present in the walls of the microtubule lattice. This has led to the general model that XMAP215 proteins promote polymerization by delivering soluble tubulin to the growing plus end, and two distinct models have been proposed to explain the mechanism. The 'concentrating reactants' model proposed previously by the authors suggests that TOG domains grab hold of tubulin in solution and concentrate at the microtubule end. The 'polarized unfurling' model proposed by the Al Bassam lab suggests that XMAP215 delivers multiple tubulins to the end, using a step-wise mechanism involving different roles for each TOG domain. The current study seeks to improve our understanding of the mechanism by developing a quantitative model to explain the binding and release of tubulins, the number of Stu2 molecules at the end, and the overall rate of tubulin addition. The authors accomplish this goal using new experimental data. The final model fills in new details of the mechanism. The authors draw a comparison between Stu2 and the actin polymerase, which bears similarity to Ena/VASP, and suggest a convergent strategy for cytoskeletal polymerases.

Strengths:

This is a focused and clearly written study that incorporates prior knowledge of XMAP215 and draws inspiration from the actin field. The data are clear and convincing, and the study accomplishes its goal of generating a new, quantitative model for Stu2. The model will be important for microtubule researchers to predict and test key points for altering XMAP215 activity across different organisms and potentially for different tubulin substrates. The comparison to Ena/VASP may also inspire similar comparisons across other microtubule and actin regulators, which could lead to new insights across the cytoskeletal fields.

Weaknesses:

The study is without major weaknesses, but there are several minor weaknesses worth noting. One is that the final model provides new details regarding the Stu2 mechanism, but does not provide a major new advance in our understanding of how the polymerase works. For example, the discussion does not clearly argue for whether the new results and model rule out either of the prior models. This appears consistent with the 'concentrating reactants' model, but does it clearly rule out the 'polarized unfurling' model? A second minor weakness is that the comparison to Ena/VASP is not developed at a deep level based on the final model. I found these ideas exciting and want more critical consideration here, but perhaps it is better suited for a commentary piece to follow.

https://doi.org/10.7554/eLife.107818.1.sa0